

See discussions, stats, and author profiles for this publication at: <https://www.researchgate.net/publication/228670176>

# Photoinduced electron transfer between anionic fluorophores and methyl viologen in homogeneous and microheterogeneous media

ARTICLE *in* JOURNAL OF LUMINESCENCE · JULY 2012

Impact Factor: 2.72 · DOI: 10.1016/j.jlumin.2012.05.001

---

READS

62

## 5 AUTHORS, INCLUDING:



**Tarak Nath Burai**

University of Akron

9 PUBLICATIONS 73 CITATIONS

SEE PROFILE



**Debashis Panda**

Rajiv Gandhi Institute of Petroleum Techno...

21 PUBLICATIONS 401 CITATIONS

SEE PROFILE



**E Siva Subramaniam Iyer**

Hebrew University of Jerusalem

11 PUBLICATIONS 61 CITATIONS

SEE PROFILE

**Anindya Datta**

Indian Institute of Technology Bombay

86 PUBLICATIONS 2,086 CITATIONS

SEE PROFILE



# Photoinduced electron transfer between anionic fluorophores and methyl viologen in homogeneous and microheterogeneous media

Tarak Nath Burai, Debashis Panda, E Siva Subramaniam Iyer, Anindya Datta\*

Department of Chemistry, Indian Institute of Technology Bombay, Powai, Mumbai 400 076, India

## ARTICLE INFO

### Article history:

Received 1 February 2012

Received in revised form

18 April 2012

Accepted 4 May 2012

Available online 6 June 2012

### Keywords:

PET

Chlorin  $p_6$

Lucifer Yellow

Micelle

Ultrafast dynamics.

## ABSTRACT

The rate and extent of photoinduced electron transfer change significantly as a result of confinement in nanovolumes. Study of such processes is an active area of research in physical chemistry. The effect is most interesting when the molecules that participate in PET are charged. In the present article, the modulation of PET has been studied for two anionic fluorophores: Lucifer Yellow CH and chlorin  $p_6$  with Methylviologen dication. PET, manifested in the quenching of fluorescence of the fluorophores, has been modulated by incorporating the molecules in organized assemblies like micelles, reverse micelles and supramolecular hosts. The dynamics of the process has been monitored in the femtosecond to nanosecond timescale. The modulation of the electron transfer has been found to be occurring mainly due to the disruption of contact ion pairs formed between the fluorophores and the quencher.

© 2012 Elsevier B.V. All rights reserved.

## 1. Introduction

In the light of increasing demand for miniaturization, chemistry plays an important role in the so called bottom up approach [1] for development of molecular devices like sensors [2], motors [3], multiplexers [4], switches [5,6], etc. Photoinduced electron transfer is a key photophysical process that is often exploited in these endeavors [7–9]. This provides the motivation for the study of PET in organic system in organized assemblies [10]. The emphasis of such studies is on generation of long lived charge separated ion pairs so that the energy produced can be used fruitfully. Encapsulation in organized assemblies can bring the donor and acceptor together for efficient forward electron transfer, followed by suppression of the back electron transfer by virtue of the microheterogeneity of the medium [11,12], PET can be either intermolecular or intramolecular. For intramolecular PET, the donor and acceptor are covalently linked to each other, usually with a spacer connecting them. Intermolecular PET is limited by rate of diffusion of molecules. It is well established that dynamics of many chemical processes are altered significantly in organized assemblies [13–18]. In reverse micelles, for example, the efficiency of charge transfer and energy transfer are influenced by the size of the water pool, location, orientation and charge of the reverse micelle [19–23].

At this point, it is useful to recapitulate the fundamental aspects of electron transfer (ET) [24–26]. A simplified form of the rate constant of ET, as proposed by Marcus, is

$$k_{ET} = \nu \exp \left[ \frac{-(\Delta G^\circ + \lambda)^2}{4\lambda k_B T} \right]$$

where  $\nu$  is the frequency of the motion in the reactant potential well,  $\lambda$  is the composite of solvent and intramolecular reorganization energy,  $-\Delta G^\circ$  is the free energy change for the overall process and  $k_B$  is the Boltzman constant. It is apparent from the expression that with increase in  $-\Delta G^\circ$ , the rate constant initially increases, reaches a maximum at  $-\Delta G^\circ = \lambda$  and then decreases when  $-\Delta G^\circ$  exceeds the reorganization energy. The cross over from increase to decrease of  $-\Delta G^\circ$  is called Marcus inversion. Such phenomenon is observed in an intramolecular process or in restricted media [14–16].

In the present work, PET between two anionic fluorescent molecules and cationic methyl viologen has been studied, in microheterogeneous media as well as in neat solutions. The two electron donors are Lucifer Yellow CH (LYCH) and chlorin  $p_6$  (Fig. 1). LYCH (Fig. 1), is a useful fluorescent label and polarity marker [27–31]. Its photophysics is governed by interplay of ISC, chain dynamics and excited state proton transfer [32,33]. The interaction of chlorin  $p_6$  with surfactant assemblies, proteins and protein surfactant aggregates has been studied extensively in the last eight years [34–41], Methylviologen dication ( $MV^{2+}$ ) (Fig. 1) is known for its diverse applications, such as an herbicidal and toxicological agent [42,43], and as an electron-accepting agent in photochemical and photoelectrochemical devices [44–46]. In our

\* Corresponding author. Tel.: +91 22 2576 7149; fax: +91 22 2576 7152.  
E-mail address: [anindya@chem.iitb.ac.in](mailto:anindya@chem.iitb.ac.in) (A. Datta).

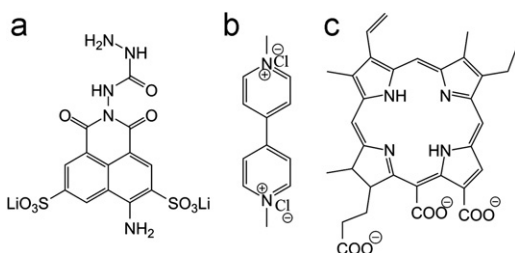


**Fig. 1.** Molecular structure of (a) LYCH and (b) Methyl viologen dication (c) Chlorin *p*<sub>6</sub>.

earlier studies of chlorin *p*<sub>6</sub> and MV<sup>2+</sup>, it appeared that an ultrafast component was being missed due to the limitation in time resolution of the TCSPC apparatus. This is the motivation for the present study, in which the hitherto elusive ultrafast component is explored using femtosecond fluorescence upconversion.

In order to explore the involvement of contact ion pairs (CIPs) and exploit the distance dependence of PET, the phenomenon has been studied in various environments. Oppositely charged LYCH and MV<sup>2+</sup> are expected to form CIPs, formation and sustainability of which depends on the medium. So, the experiment has been performed in solvents of differing polarity. PET has also been studied in reverse micelle and  $\beta$ -cyclodextrin ( $\beta$ -CD). It is known that MV<sup>2+</sup> forms a strong inclusion complex with  $\beta$ -cyclodextrin [47] while chlorin *p*<sub>6</sub> does not [34–41]. So, it would be interesting to explore if encapsulation of methyl viologen dication would disrupt the contact ion pair/association complex and thus lead to a slower rate of electron transfer in  $\beta$ -CD. In reverse micelle (RM), chlorin *p*<sub>6</sub> is expected to reside at the interface, irrespective of the nature of the surfactant used. Methyl viologen, being positively charged, may be expected to stick to the head group of the negatively charged RM. In RM of surfactants with positively charged or uncharged head group, on the other hand, it is more likely to reside in the water pool. It would be interesting to study the effect of such differential localization of donor and acceptor on PET.

## 2. Materials and methods.

Lucifer Yellow CH, obtained from Molecular Probes is used as received. Chlorin *p*<sub>6</sub> has been prepared from chlorophyll, extracted from spinach leaves using literature procedure [48,49]. Methyl viologen dichloride, Cetyl trimethyl ammonium bromide (CTAB) (AR grade), Triton X-100 (TX-100) (AR grade), Sodium dodecyl sulfonate (SDS) (AR grade),  $\beta$ -cyclodextrin (AR grade), from Aldrich have been used as received. Aerosol OT from Aldrich is purified by overnight stirring of a methanol solution with activated charcoal (1:20 w/w) and subsequent vacuum evaporation of the solvent [50,51]. Deionized water is distilled twice before being used as a solvent. Stock solutions of 0.1 M CTAB is prepared in a mixture of isooctane: n-pentanol::9:1 [52] and 0.27 M TX-100 reverse micelle in a mixture of benzene: n-heptane::3:1 [53]. The reverse micelles of desired *w*<sub>0</sub> are prepared by adding required amount of water. The concentration of SDS,  $\beta$ -CD, are maintained at 14 mM, 5 mM respectively.

The absorption and fluorescence spectra are recorded on JASCO V-530 spectrophotometer and Varian Cary Eclipse fluorimeter, respectively. The excitation wavelength ( $\lambda_{ex}$ ) is 430 nm for fluorescence measurements. The absorbance at this wavelength is kept below 0.1, in order to avoid inner filter effects. Fluorescence quantum yields ( $\phi_f$ ) are calculated after proper correction for changes in absorbance using literature value of C153 [54]. Time-resolved fluorescence measurements are performed using a

picosecond pulsed diode laser based TCSPC fluorescence spectrometer with  $\lambda_{ex}$ =406 nm. The emission from the samples is collected at right angle to the direction of the excitation beam, at magic angle polarization (54.7°), except for the anisotropy measurements. The full width at half maximum of the instrument response function is 250 ps for 406 nm. The data are fitted to multiexponential functions after deconvoluting the instrument response function by an iterative reconvolution technique, using the IBH DAS 6.2 data analysis software, where reduced  $\chi^2$  and weighted residuals serve as parameters for goodness of fit [55]. The femtosecond upconversion experiment is performed on the FOG 100 spectrometer from CDP Corporation, Russia. The LYCH is excited at 415 nm obtained from the second harmonic of a mode-locked Tisapphire laser (Tsunami, Spectra Physics) pumped by 5 W Millennia (Spectra Physics). The fundamental beam is frequency doubled in a nonlinear crystal (1 mM BBO,  $\theta$ =25°,  $\phi$ =90°). The fluorescence emitted from the sample is upconverted in a nonlinear crystal (0.5 mM BBO,  $\theta$ =38°,  $\phi$ =90°) using a gate pulse of the fundamental beam. The upconverted light is dispersed in a monochromator and detected using photon counting electronics. A cross-correlation function is obtained using the scattering from ethanol. It displays a full width at half maximum (FWHM) of 350 fs. The femtosecond fluorescence transients are fitted using a Gaussian shape for the excitation pulse. To fit the femtosecond data the long decay components which we need, is taken from TCSPC experiment [56].

The time-dependent anisotropy,  $r(t)$  is constructed from the decays at parallel and perpendicular directions to that of the excitation polarization polarization ( $I_{||}(t)$  and  $I_{\perp}(t)$  respectively) as:

$$r(t) = \frac{I_{||}(t) - I_{\perp}(t)}{I_{||}(t) + 2I_{\perp}(t)} \quad (1)$$

The decays of  $r(t)$  are fitted to single and multiexponential functions as required, using the formula

$$r(t) = r_0 \sum_i a_i \exp(-t/(\tau_i)) \quad (2)$$

For all the fluorescence measurements, the optical density (OD) of the solutions have been kept quite low (<0.2) at the excitation wavelength.

## 3. Results and discussion

The addition of methyl viologen (MV<sup>2+</sup>) to fluorophore Lucifer Yellow CH (LYCH) leads to a broadening of absorption spectrum (Fig. S1a). This feature is signature of ground state interaction [36]. The reason can be attributed to the electrostatic interaction between MV<sup>2+</sup> cation and anionic form of LYCH. The fluorescence maximum, which occurs at 537 nm in aqueous solution, gets blue shifted by 5 nm in the presence of 10 mM MV<sup>2+</sup> (Fig. S1b). This increase in energy gap is likely due to stabilization of ground state, due to association with MV<sup>2+</sup>. The spectral shift is accompanied with a significant decrease in quantum yield. Given the nature of interacting species, the non radiative process can be ascribed to PET. The Stern–Volmer plot is non-linear and has a downward curvature (Fig. 2(a)). Such a phenomenon is usually observed under circumstances where only a fraction of fluorophore is in the vicinity of quencher [57,58]. A linear variation for  $F_0/\Delta F$  with inverse of quencher concentration, i.e. a linear shape of the modified Stern–Volmer plot (Fig. 2(b)), implies that MV<sup>2+</sup> quenches a fraction of fluorophores and another fraction is inaccessible to the quencher. In the system under study, such fractional accessibility can arise due to the formation of contact

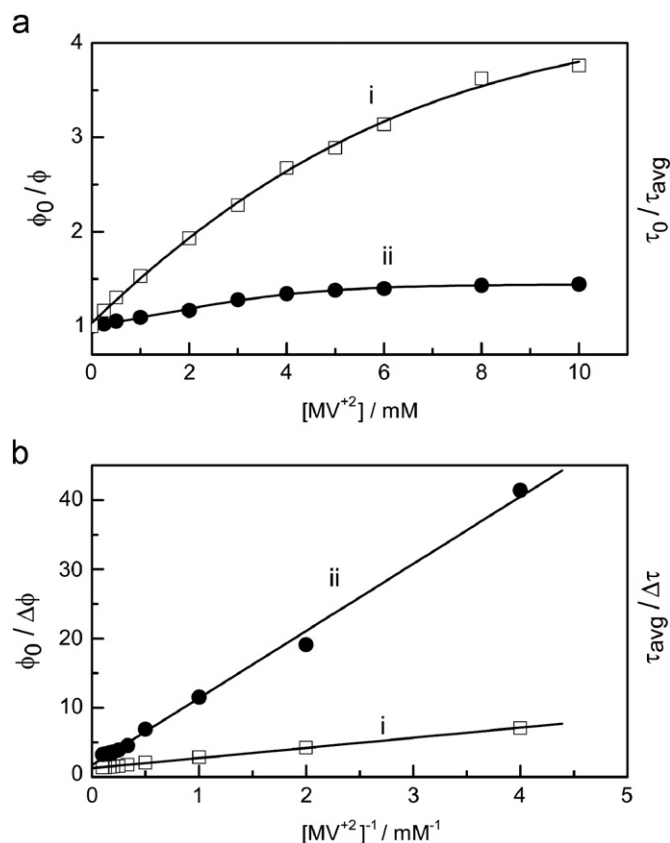


**Fig. 2.** (a) Stern–Volmer plot and (b) the modified Stern–Volmer plot of LY CH in presence of methyl viologen in water: (i) fluorescence quantum yield ( $\phi_0/\phi$ ;  $\phi_0/\Delta\phi$  respectively) and (ii) fluorescence lifetime ( $\tau_0/\tau_{avg}$ ;  $\tau_{avg}/\Delta\tau$  respectively).

ion pairs (CIPs), which would hinder further approach of the positively charged quencher molecules at higher concentration.

The fluorescence decay of LYCH in water is single exponential with a lifetime of 5 ns (Fig. S1c, Table S3). Upon addition of  $MV^{2+}$  a short component of 2 ns appears. The contribution of this component increases upon increasing the concentration of the quencher. This indicates the presence of the fluorophore in two different states or environments. Contribution from one of them increases at the cost of the other. The short component may be assigned to the CIP. The longer component matches that of LY CH in water in absence of the quencher and hence is assigned to unquenched LYCH molecules. In recent past, a similar observation is also made with quenching of fluorescence of Chlorin  $p_6$  by  $MV^{2+}$  [34]. The Stern–Volmer constant obtained from time resolved measurements is significantly lower than the values obtained from steady state measurement (Table 1). This observation indicates that a major part of the quenching is ultrafast in nature.

In order to probe the involvement of contact ion pairs in the PET, similar experiments are performed in methanolic medium. Methanol being less polar than water, CIPs are expected to be dissociated to a lesser extent in these solvents. This might lead to a further discrepancy between Stern–Volmer constants obtained from steady state and time-resolved experiments. Stern–Volmer constants calculated from the slope of the initial parts the Stern–Volmer plots are presented in Table 1. It is evident that the fluorescence quenching occurs to a significantly greater extent in methanol. Stern–Volmer constants obtained from time resolved measurements are markedly lesser than those obtained from plots of fluorescence quantum yields. Notably, the difference between the Stern–Volmer constants obtained from the steady

**Table 1**

Comparison of Stern–Volmer constant  $K_{SV}$  and bimolecular quenching constant  $k_q$  for quenching of LY CH by  $MV^{2+}$  in water, methanol, and TX-100, CTAB, AOT reverse micelle from steady state and time resolved experiments using average lifetimes.

Medium	Steady state <sup>a</sup>		Time resolved	
	$K_{SV}$ (l M <sup>-1</sup> )	$k_q$ (l M <sup>-1</sup> s <sup>-1</sup> )	$K_{SV}$ (l M <sup>-1</sup> )	$k_q$ (l M <sup>-1</sup> s <sup>-1</sup> )/10 <sup>10</sup>
Water	863	17.3	175	3.5
Methanol	3713	44.4	250	3.0
AOT ( $w_0=4$ )	2031	38.4	338	6.4
AOT ( $w_0=16$ )	309	5.1	126	2.5
CTAB ( $w_0=12$ )	235	3.7	167	2.6
CTAB ( $w_0=32$ )	135	2.1	71	1.1
TX-100 ( $R=5$ )	1678	19.0	719	8.1

<sup>a</sup> The values of  $k_q$  obtained from the steady state experiments are not correct because they are dominated by the static quenching.

state and time resolved data is more prominent in methanol, where CIPs are expected to form to a greater extent than in aqueous solutions, by virtue of the lower dielectric constant of methanol compared to that of water. This observation supports the contention of the quenching being ultrafast in nature and that of the involvement of CIPs, as is the case in some other oppositely charged donor–acceptor systems in homogeneous solutions [59]. The picosecond experiments result in a much lower value of  $K_{SV}$  than the values obtained from steady state experiments, indicative of an ultrafast process missed in the timescale of the experiment. The bimolecular quenching constants obtained from steady state and time resolved experiments are significantly different. This can be attributed to the fact that the fluorescence is dominated by the static quenching and the relationship  $K_{SV}=k_q\tau$  does not hold and hence the values from time resolved measurements should be considered. In order to probe this, the femtosecond fluorescence upconversion studies have been performed to explore the ultrafast dynamics of PET. In the absence of  $MV^{2+}$ , LYCH exhibits wavelength-dependent fluorescence decays, with a rise at the red end in water and MeOH. This wavelength dependence is associated with solvation dynamics [60]. We observe that in water, methanol, AOT reverse micelles at lower water contents and in TX-100 the  $k_q$  obtained from time resolved experiments are significantly smaller than the ones obtained from steady state experiments. This indicates that the CIP formed together are held closely in and the quenching is static. In fact, in such a case,  $k_q$  has no physical meaning, as  $K_{SV}$  is simply the binding constant and cannot be written as a product of the bimolecular quenching constant and lifetime of the unquenched fluorophore. However in the case of CTAB and larger reverse micelles of AOT the quenching is dynamic in nature. Moreover the bimolecular quenching rate constant is larger than the orders of diffusion controlled limit. Such phenomenon is usually observed when the electrostatic forces of attraction between the donor and the acceptor significant [61]. Upon addition of  $MV^{2+}$  the fluorescence decays of the LYCH in MeOH become very fast (Fig. 3, Table S1). However no rise time is observed as in case of quencher free medium. The absence of the rise at the red end indicates that electron transfer is faster than the solvation time of 6 ps [62]. A similar phenomenon has been reported previously for coumarin derivatives in micellar media [63]. In the presence of 6 mM  $MV^{2+}$ , a 1 ps component is observed, with amplitude of 50%, along with the 10 ps decay and the long component present in absence of quencher. This suggests that ultrafast electron transfer occurs in  $\leq 10$  ps time scale. In the presence of 6 mM  $MV^{2+}$  in water, contribution of 1.5 ps component increases at 530 nm. Analogous to in MeOH, the risetime at the red end i.e. at  $\lambda_{em}=608$  nm, is no longer observed at a very high  $MV^{2+}$  concentration (Fig. 3).

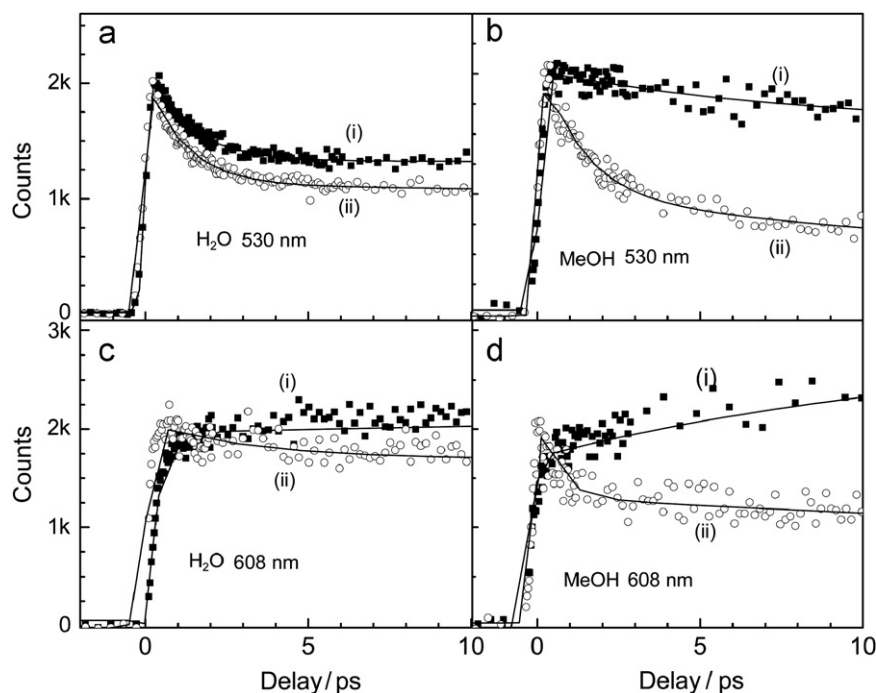


**Fig. 3.** Femtosecond transients of LYCH in MeOH at (a)  $\lambda_{em}=530$  nm, (b)  $\lambda_{em}=608$  nm, and water at (c)  $\lambda_{em}=530$  nm, (d)  $\lambda_{em}=608$  nm at  $MV^{2+}$  concentrations of (i) 0 mM (ii) 6 mM respectively.

This suggests that in water, PET is faster than solvation. Notably, the content of ultrafast quenching is significantly more than in water (Fig. 3). This observation further supports the involvement of CIPs which form to a greater extent in methanol than in aqueous solution.

The fact that microheterogeneous media can bring about significant changes in the photochemistry of molecules invokes the need to study these processes in such media. The photoinduced electron transfer between LYCH and  $MV^{2+}$  has been studied in the water pools of *n*-heptane/AOT/water microemulsion, in order to understand the changes brought about in the process as a result of confinement. Our previous experiments have shown that LYCH does not interact with micelles formed by SDS and TX-100, which is evident from the fact that there is no change in spectral features. However marked changes are seen with CTAB. This has been explained in the light of the electrostatic interactions. The quantum yields obtained from steady state and time resolved experiments show that the quenching is substantially static [32]. The absorption spectra, in the reverse micelles resemble that in water, except in the red edge. Beyond  $w_0=24$ , the absorption and fluorescence spectra resemble the spectra recorded in the bulk aqueous solutions (Fig. S3a). This indicates that LYCH indeed resides in the core of the water pool of the RM, as may be expected from its highly polar nature. The fluorescence quantum yield increases by a factor of 4.5 upon increase the  $w_0=0$  to 24. The addition of  $MV^{2+}$  to LYCH in AOT reverse micelles produces no significant difference in the LYCH absorption spectrum. This indicates that there is no ground state association between the fluorophore and the quencher in these reverse micelles. However, the fluorescence spectrum gets narrowed and exhibits a maximum at 542 nm (Figure S3b). The fluorescence quenching by methyl viologen is found to become less efficient with increase in  $w_0$  (Figure S4, Table 1). This reflects an increase in the donor–acceptor distance upon increasing the water content, which may be rationalized as follows; LYCH, being strongly hydrophilic, resides in the water pool where the positively charged  $MV^{2+}$  sticks to the anionic head groups of the surfactant. The difference

between the Stern–Volmer constant using steady state and time resolved data is significant at low water content, but small in higher content (Table 1). This is an evidence of close association of the donor and the acceptor in the first case, whereby CIPs are formed and static quenching predominates. At higher water contents, however static quenching is decreased due to the separation between the donor and acceptor as would arise out of the proposed model. A look at the time resolved (TCSPC) data reveals that the fluorescence decay of LYCH in AOT reverse micelle is tri-exponential. The longer time constant is 7.74 ns with amplitude 46% while two other components are 3 ns and 570 ps with amplitudes 28% and 26% respectively, which indicates a spatial distribution of fluorophore in microemulsion (Fig. S7, Table S4).

At  $w_0=4$ , the decay becomes single exponential with a time constant 5.30 ns which suggest that LYCH is confined exclusively in the water pool. At higher concentration of quencher (2–4 mM) at  $w_0=4$  the decay becomes tri-exponential with a 200 ps component with amplitude 0.40 (Fig. S7 and Table S3). This fast component may be ascribed to the PET. In order to explain the discrepancies of steady state and TCSPC measurements the experiments are performed at finer time scales using femtosecond fluorescence upconversion. We observe that the decays at  $w_0=4$  and 8 are indistinguishable. We observe a 2 ps component at 530 nm in both, absence as well as presence of quencher. The rise time at the red end, originating from solvation dynamics, is reduced upon addition of  $MV^{2+}$  (Table S1).

With the observations of ultrafast experiments in LYCH and the steady state and TCSPC results of Clp6-  $MV^{2+}$  we proceed towards the ultrafast quenching owing to PET between chlorin  $p_6$  and  $MV^{2+}$  in water. It has been investigated by the femtosecond fluorescence upconversion at  $\lambda_{em}=666$  nm. In water 32 ps component (27%) in absence of  $MV^{2+}$  is quenched to 3 ps (0.76%) in presence of 0.5 mM  $MV^{2+}$ . This ultrafast quenching was not observed in TCSPC experiment reported earlier due to limitation of the instrumental resolution. This by and large accounts for the drastic difference in the Stern–Volmer constants obtained by time



resolved and steady state measurements. The absorption and emission spectra of chlorin  $p_6$  in AOT reverse micelle do not change with increase in water content of the water pool of the reverse micelle (Fig. S5). This indicates that hydrophobicity and polarity do not affect the photophysics of chlorin  $p_6$ . So we have observed the fluorescence quenching on only  $w_0=8$ . From Stern–Volmer quenching constant it is observed that the quenching efficiency is very small in this medium (Table S5). This is likely to be because unlike the highly polar LY CH, chlorin  $p_6$  is likely to be located near the head group, like  $MV^{2+}$ . So, the movements of both the donor and the acceptor are restricted, thereby reducing the quenching efficiency. For chlorin  $p_6$  value of Stern–Volmer constant is  $68 \text{ l mole}^{-1}$  at  $w_0=8$ . The fluorescence decays of chlorin  $p_6$  in aqueous solution exhibit no change on addition of  $MV^{2+}$  indicating only static quenching is operative here. This can be apparently explained in the light of instantaneous electron transfer between  $MV^{2+}$  and chlorin  $p_6$  in restricted movement inside of water pool on reverse micelle. This confirms that in AOT reverse micelle, only static quenching is operative. The upconversion experiments in AOT reverse micelle at  $w_0=8$ , decay is associated with short component of 16 ps with amplitude 10% in absence of quencher (Fig. 4, Table 3).

In order to explore the viability of this contention, the study has been extended to neutral and cationic reverse micelles.

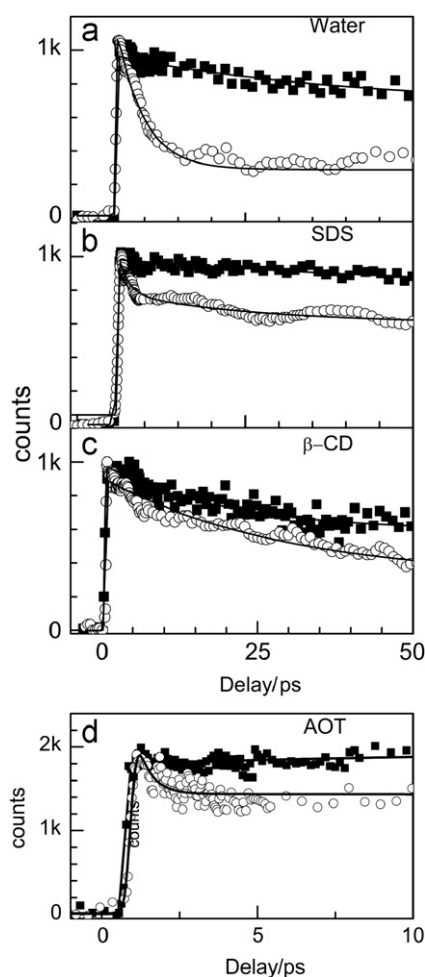


**Fig. 4.** Femtosecond transients of chlorin  $p_6$  in (a) water, (b) 14 mM SDS, (c) 5 mM  $\beta$ CD, in absence and presence of methyl-viologen 0.50 mM and 3 mM respectively, and (d)  $w_0=8$  in  $MV^{2+}$  concentration 0 mM, 6 mM at  $\lambda_{ex}=405 \text{ nm}$  at  $\lambda_{em}=665 \text{ nm}$ .

The Stern–Volmer plots are shown in Fig. S4. This signifies that fluorophore is quenched by dynamic quenching process supported by time-resolved measurements. Quenching of fluorescence of LYCH by  $MV^{2+}$  is observed in CTAB reverse micelles at lower water content. The efficiency is less than that in water, seemingly due to the electrostatic interaction between the negatively charged LY CH and the positively charged head-groups of the CTAB cations. Such an interaction has been observed in aqueous CTAB micelles [32]. At higher water contents ( $w_0=32$ ), the quenching is found to be almost negligible (Table 1). This is in similar to the observation of less efficient quenching in AOT reverse micelles at higher water content where the electrostatic attraction between  $MV^{2+}$  and the headgroup of surfactant decreases the quenching efficiency. In surfactants with positively charged headgroups, similar electrostatic attraction between LYCH and the surfactant is operative. So, the steady state experiments in AOT and CTAB reverse micelles are in line with each other and indicate the important role of change of the surfactant headgroup as well as the water content in determining the efficiency of the PET between oppositely charged donors and acceptors. The quenching is found to be way more efficient in TX-100 reverse micelle at  $w_0=5$  than in CTAB reverse micelle ( $w_0=12$ ) (Table 2). This further establishes the formation and subsequent decrease in quantum yield due to formation of contact ion pairs. Stronger CIP are formed in case of TX-100 because in this case neither the fluorophore nor the quencher interacts with the surfactant. For LY CH in TX-100 reverse micelle ( $w_0=5$ ) in presence of  $MV^{2+}$ , component of 8.86 ns and 1.4 ns are observed. With increasing concentration of  $MV^{2+}$  the 1.4 ns component remains unchanged. However, the contribution of long component decreases and that of 1.4 ns component increases to 60% at 3 mM  $MV^{2+}$ . This clearly indicates that as the concentration of quencher is increased more quencher is in vicinity of fluorophores and is not affected by the surfactant. In CTAB reverse micelle at  $w_0=12$ , the amplitude of short component increases and that of long component decreases (Fig. S6, Table S3). Analogous to AOT, in the presence of 6 mM  $MV^{2+}$  in CTAB reverse micelle, contribution of 5 ps component increases to 33% at  $\lambda_{em}=530 \text{ nm}$ . While in TX-100 reverse micelle 80 ps component with contribution 10% is quenched to 22 ps having contribution of 40% (Fig. S6, Table S3). The risetime of LY CH in both reverse micelles is quenched at the red end i.e. at  $\lambda_{em} 600 \text{ nm}$  at a very high  $MV^{2+}$  concentration. However it does not vanish completely.

The modulation of PET due to incorporation in supramolecules has been explored. In the present case the experiment has been performed in cyclodextrins ( $\beta$ -CD). It is earlier reported that the fluorescence quantum yield ( $\phi_f$ ) of chlorin  $p_6$  does not exhibit any change on addition of  $\beta$ -CD indicating that there is no interaction of the fluorophores with  $\beta$ -CD. The absorption peaks of chlorin  $p_6$  in 5 mM  $\beta$ -CD aqueous solution get red shifted and broadened with gradual addition of  $MV^{2+}$  indicating ground state association due to their opposite charges [64]. The changes in absorption spectra on addition of  $MV^{2+}$  to chlorin  $p_6$  in 5 mM  $\beta$ -CD aqueous solution are less prominent than in bulk water (Fig. 5). This indicates that the extent of contact ion pair formation is reduced substantially in host compared to neat aqueous solutions. A linear Stern–Volmer plot, with a steeper slope in  $\beta$ -CD solution is observed than that in neat aqueous solution (Fig. 5a, Table S5). The fluorescence decays of chlorin  $p_6$  in  $\beta$ -CD aqueous solution exhibit no change on addition of  $MV^{2+}$  indicating only static quenching is operative here as in water (Fig. 5c). This can be also explained in the light of instantaneous electron transfer in the association complexes between  $MV^{2+}$  and chlorin  $p_6$ . So by steady state and TCSPC technique it is observed that there is no change of the mechanism of electron transfer in water and  $\beta$ -CD media. From the difference in steady state nature, it is expected to be observed

**Table 2**Fluorescence decay parameters of LYCH in Reverse Micelle at different concentration of  $MV^{2+}$ .

Medium	$[MV^{2+}]/\text{mM}$	$\lambda_{em}/\text{nm}$	$\tau_1/\text{ps}$	$\tau_2/\text{ps}$	$\tau_3/\text{ps}$	$a_1$	$a_2$	$a_3$
CTAB reverse micelles ( $w_0=12$ )	0	530	4750		6.29	0.87		0.13
	6	530	5000	1260	4.31	0.44	0.23	0.33
	0	600	3700		6.50	1.20		–0.20
	6	600	2650	1260	4.50	0.69	0.36	–0.05
	0	530	8860		80	0.90		0.10
TX-100 Reverse micelles ( $R_0=5$ )	2	530	6270	1300	22	0.29	0.31	0.40
	0	600	9000		90	1.20		–0.20
	2	600	6300	1350	5	0.51	0.53	–0.04

**Table 3**Fluorescence decay parameters of chlorin  $p_6$  in water, SDS micelle,  $\beta$ -CD in water and AOT reverse micelle at  $w_0=8$  at difference concentration of bulk  $MV^{2+}$  concentration.  $\lambda_{ex}=406\text{ nm}$ .

Medium	$[MV^{2+}]/\text{mM}$	$\tau_1/\text{ps}$	$\tau_2/\text{ps}$	$\tau_3/\text{ps}$	$\tau_4/\text{ps}$	$a_1$	$a_2$	$a_3$	$a_4$	$\langle \tau \rangle / \text{ps}$
Water	0		32	3600			0.27	0.73		2673
	0.5		3	3600			0.76	0.24		866
14 mM SDS micelle	0		60	3100	4200		0.17	0.40	0.43	
	0.5	0.5	20	2000	4200	0.16	0.15	0.26	0.43	
5 mM $\beta$ -CD	0		18	3290			0.38	0.62		2049
	0.5		18	3010			0.56	0.44		1335
AOT reverse micelle ( $w_0=8$ )	0	16		3500		0.10		0.90		3500
	6	0.50		3000		0.40		0.60		1800

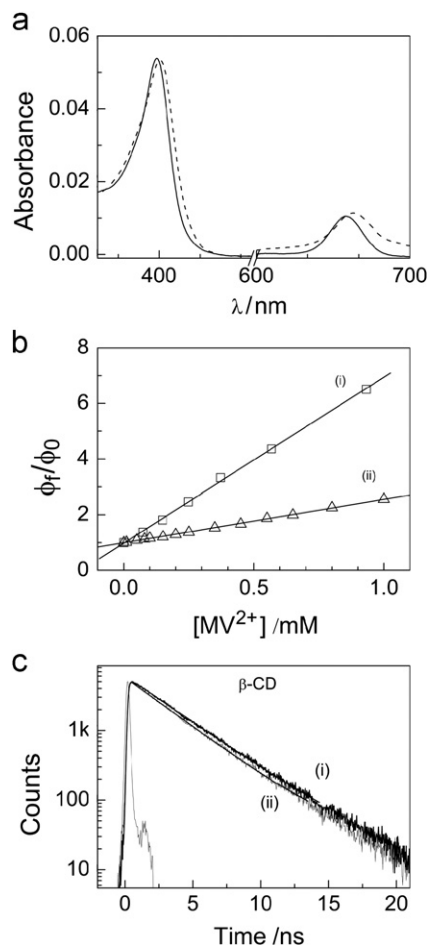


**Fig. 5.** (a) Principal absorption peaks of chlorin  $p_6$  in the absence (solid line) and presence (dotted line) of 1 mM  $MV^{2+}$  in 5 mM  $\beta$ -CD. The Q bands have been magnified for the sake of clarity. The concentration of chlorin  $p_6$  is  $4 \times 10^{-6}\text{ M}$ . (b) The Stern–Volmer plots with fluorescence quantum yields ( $\phi_f$ ) of  $4 \times 10^{-6}\text{ M}$  chlorin  $p_6$  in (i) 5 mM  $\beta$ -CD (ii) water. (c) Fluorescence decay of  $4 \times 10^{-6}\text{ M}$  chlorin  $p_6$  in the (i) absence and (ii) presence of 1 mM  $MV^{2+}$  in 5 mM  $\beta$ -CD. The IRF (FWHM=250 ps) are shown in dashed lines.

different mechanism in water and  $\beta$ -CD. That why we have use femtosecond upconversion technique which is later discussed. Before discussing this upconversion result we have also observed the effect of hydrophobicity on the photoinduced electron transfer. The ultrafast PET between chlorin  $p_6$  and  $MV^{2+}$  has been investigated by the femtosecond fluorescence upconversion at  $\lambda_{em}=666\text{ nm}$ , in water, SDS micelle, AOT reverse micelle and  $\beta$ -CD (Fig. 4). Ultrafast dynamic quenching is observed in water. In water 32 ps component (27%) in absence of  $MV^{2+}$  is quenched to 3 ps (0.76%) in presence of 0.5 mM  $MV^{2+}$ . This ultrafast quenching was not observed in TCSPC experiment reported earlier due to limitation of the instrumental resolution.

In presence of 6 mM  $MV^{2+}$  this is decreased to an ultrafast component (0.5 ps). This result is consistent with static quenching observed from the steady state experiment. The rate of the electron transfer has been calculated by using following equation where  $\tau_0$  and  $\tau$  are the lifetime of the donor in absence and presence of the quencher  $MV^{2+}$ . We have use the average lifetime in presence of the quencher. Unlike in SDS media and water, in  $\beta$ -CD solution, the relative contribution of the 18 ps component increases to 56% in presence of 0.5 mM  $MV^{2+}$  from 38% in absence of  $MV^{2+}$ . It is readily seen that there is a significant change in the initial part of the decay in SDS micelle and water while the corresponding change is smaller in supramolecular host [65].

$$\frac{1}{\tau} = \frac{1}{\tau_0} + k_{ET}[Q] \quad (3)$$

The ultrafast photoinduced electron transfer has been observed in SDS micelle. This faster ET process indicates the stability and feasibility of more number of contact ion pair. If ion pair is formed rotational motion will be also affected. So we looked at anisotropy study. In chlorin  $p_6$ , different anisotropic behavior has been observed. The bi-exponential anisotropy decay in micelle solution is often expressed by a two step model considering the three motions, namely; wobbling motion, the lateral diffusion, and rotational motion of the micelle [66,67]. In our proposed model for fluorescence quenching, only one component of the lifetime should exhibit a decrease on addition of  $MV^{2+}$  and the other, corresponding to unavailable fluorophores,

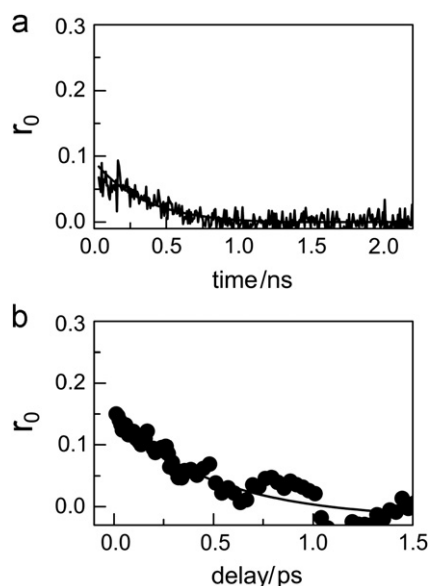


**Fig. 6.** Fluorescence anisotropy decay ( $\lambda_{ex}=405$  nm) of chlorin  $p_6$  ( $\lambda_{em}=665$  nm) in (a) 14 mM SDS (from TCSPC data), (b) SDS micelle with 0.5 mM  $MV^{2+}$  (from Upconversion experiment). The points denote the actual values of anisotropy and the solid lines denote the best fit to the experimental data.

should remain unchanged. From TCSPC experiment we have seen that in SDS micelle, the anisotropy decay (Fig. 6) is quite fast ( $\sim 200$  ps) and single exponential, with initial anisotropy.

The observed decay is due to the chlorin  $p_6$  molecules bound to the micelles. Free chlorin  $p_6$  is responsible for ultrafast decay, which goes undetected in this experiment and leads to an  $r_0$  value of 0.02. Lateral diffusion of the probe does not occur, as is indicated by the absence of its characteristic component of 700–800 ps. The ultrafast component of the fluorescence anisotropy has been measured using upconversion setup. It is interesting that rotational diffusion time is 0.4 ps which is comparable to the ultrafast decay component of ET ( $\sim 0.5$  ps) in micelle. This indicates that the observed ultrafast ET process in SDS micelle is significantly influenced by the orientational motion of the reactants in the micelles.

#### 4. Conclusions

The fluorescence quenching studies of Lucifer Yellow CH and chlorin  $p_6$  by methylviologen dication in homogeneous and heterogeneous media reveal that both static quenching and dynamics quenching occurs. The extent of the one having a greater contribution over other is dependent upon the medium, and by molecules in the immediate vicinity of the quencher or fluorophore or both. We observe that static quenching is dominating in case of quenching of LYCH in neat solutions like water and methanol. In case of reverse micelles like AOT and CTAB the quenching is dynamic. Similar observations are made in Chlorin  $p_6$  quenching experiments. Though the features of static quenching are similar for both the fluorophores the dynamics are vastly different and are apparent from the upconversion studies. The anisotropy experiments indicate that orientation plays significant role in fluorescence quenching in case of chlorin  $p_6$  while no contribution in case of LYCH. The experiments signify that PET process can be manipulated by changing the medium and external agents like supramolecules. These observations pave the way for development of novel systems which might be used in for the development of molecular devices.

#### Acknowledgment

The authors thank DST, India and CSIR for funding. ESSI, TNB, DP thank CSIR for SRFship.

#### Appendix A. Supporting information

Supplementary data associated with this article can be found in the online version at <http://dx.doi.org/10.1016/j.jlumin.2012.05.001>.

#### References

- [1] V. Balzani, A. Credi, F.M. Raymo, J.F. Stoddart, *Angew. Chem.* 112 (2000) 3348.
- [2] Z. Huang, J. Du, J. Zhang, X.-Q. Yu, L. Pu, *Chemical Commun.* 48 (28) (2012) 3412.
- [3] M.M. Polalrd, M. Lubomska, P. Rudolf, B.L. Feringa, *Angew. Chem. Int. Ed.* 46 (2007) 1278.
- [4] S.D. Straight, J. Andreasson, G. Kodis, S. Bandhopadhyay, R.H. Mitchell, T.A. Moore, A.L. Moore, D. Gust, *J. Am. Chem. Soc.* 127 (2005) 9403.
- [5] H. Tian, B. Qin, R. Yao, X. Zeaho, S. Yang, *Adv. Mater.* 15 (2003) 2104.
- [6] M. Suresh, A. Ghosh, A. Das, *Tetrahedron Lett.* 48 (2007) 8205.
- [7] A.-G. Griesbeck, N. Hoffmann, K.-D. Warzecha, *Acc. Chem. Res.* 40 (2007) 128.
- [8] A.E. Bragg, B.J. Schwartz, *J. Phys. Chem. A* 112 (2008) 3530.
- [9] S. Iwai, S. Murata, M. Tachiya, *J. Chem. Phys.* 109 (1998) 5963.
- [10] K. Kalyanasundaram, *Photochemistry in Microheterogeneous Systems*, Academic Press, London, 1987.
- [11] M. Aoudia, M.A.J. Rodgers, *J. Phys. Chem. B* 107 (2003) 6194.
- [12] D.M. Togashi, S.M.B. Costa, *Phys. Chem. Chem. Phys.* 4 (2002) 1141.
- [13] V.O. Saik, A.A. Goun, J. Nanda, K. Shirota, H.L. Tavernier, M.D. Fayer, *J. Phys. Chem.* 108 (2004) 6696.
- [14] M. Kumbhakar, S. Nath, T. Mukherjee, H. Pal, *Phys. Chem. Chem. Phys.* 7 (2005) 034705.
- [15] A. Chakraborty, D. Chakrabarty, P. Hazra, D. Seth, N. Sarkar, *Chem. Phys. Lett.* 382 (2003) 508.
- [16] A.K. Satpati, M. Kumbhakar, S. Nath, H. Pal, *J. Photochem. Photobiol. A* 200 (2008) 270.
- [17] M.K. Sarangi, S. Basu, *Phys. Chem. Chem. Phys.* 13 (2011) 16821.
- [18] S.D. Choudhury, M. Kumbhakar, S. Nath, H. Pal, *J. Chem. Phys.* 127 (2007) 194901.
- [19] D. Severino, H.C. Junqueira, M. Gugliotti, D.S. Gabrielli, M.S. Baptista, *Photochem. Photobiol.* 77 (2003) 459.
- [20] D. Grand, A. Dokutchaev, *J. Phys. Chem. B* 101 (1997) 3181.
- [21] D. Grand, *J. Phys. Chem. B* 102 (1998) 4322.
- [22] S.D. Choudhury, M. Kumbhakar, S. Nath, S.K. Sarkar, T. Mukherjee, H. Pal, *J. Phys. Chem. B* 111 (2007) 8842.
- [23] C. Harris, P.V. Kamat, *ACS Nano* 3 (2010) 682.
- [24] R.A. Marcus, *J. Chem. Phys.* 24 (1956) 966.
- [25] R.A. Marcus, *Rev. Mod. Phys.* 65 (1993) 599.
- [26] R.A. Marcus, N. Sutin, *Biochim. Biophys. Acta* 811 (1985) 265–322.
- [27] J.A. Lee, P.A.G. Fortes, *Biochemistry* 25 (1986) 8133.
- [28] C. Peracchia, *Nature* 290 (1981) 597.
- [29] S. Matsugo, S. Kawanishi, K. Yamamoto, H. Sugiyama, T. Matsuura, I. Saito, *Angew. Chem. Int. Ed. Engl.* 30 (1991) 1351.
- [30] J.E. Rogers, S.J. Weiss, *J. Am. Chem. Soc.* 122 (2000) 427.
- [31] B. Abraham, L.A. Kelly, *J. Phys. Chem. B* 107 (2003) 12534.
- [32] P.P. Mishra, A.L. Koner, A. Datta, *Chem. Phys. Lett.* 400 (2004) 128.
- [33] D. Panda, P.P. Mishra, A.L. Koner, R.B. Sunoj, A. Datta, *J. Phys. Chem. A* 110 (2006) 5585.
- [34] P.P. Mishra, J. Bhatnagar, A. Datta, *J. Phys. Chem. B* 109 (2005) 24225.
- [35] A. Datta, A. Dube, B. Jain, A. Tiwari, P.K. Gupta, *Photochem. Photobiol.* 75 (2002) 488.
- [36] T.K. Mukherjee, P.P. Mishra, A. Datta, *Photoinduced, Chem. Phys. Lett.* 407 (2005) 119.
- [37] S. Patel, *Chem. Phys. Lett.* 413 (2005) 31.
- [38] P.P. Mishra, A. Datta, *Biophys. Chem.* 121 (2006) 224.
- [39] P.P. Mishra, R. Adhikary, P. Lahiri, A. Datta, *Chlorin, Photochem. Photobiol. Sci.* 5 (2006) 741.
- [40] P.P. Mishra, S. Patel, A. Datta, *J. Phys. Chem. B* 110 (2006) 21238.
- [41] S. Patel, A. Datta, *J. Phys. Chem. B* 111 (2007) 10557.
- [42] J.S. Bus, S.D. Aust, J.E. Gibson, *Biochem. Biophys. Res. Commun.* 58 (1974) 749.
- [43] C.L. Kuhn, A.T. Bird, *Chem. Soc. Rev.* 10 (1981) 49.
- [44] J.R. Derwent, *J. Chem. Soc., Chem. Commun.* (1980) 805.
- [45] R.J. Lever, A.B.P. Crutchley, *J. Am. Chem. Soc.* 102 (1980) 7128.
- [46] S.Y. Choi, M. Mamak, N. Coombs, N. Chopra, G.A. Ozin, *Nano Lett.* 4 (2004) 1231.
- [47] K. Moon, E.A. Kaifer, *Org. Lett.* 6 (2004) 185.
- [48] A. Datta, A. Dube, B. Jain, A. Tiwari, P.K. Gupta, *Photochem. Photobiol.* 75 (2002) 488.
- [49] P.P. Mishra, J. Bhatnagar, A. Datta, *Chem. Phys. Lett.* 386 (2004) 158.
- [50] M. Wong, J.K. Thomas, M. Graetzel, *J. Am. Chem. Soc.* 98 (1976) 2391.



- [51] A. Datta, D. Mandal, S.K. Pal, K. Bhattacharyya, J. Phys. Chem. B 101 (1997) 10221.
- [52] J. Zhang, L.D. Sun, C. Qian, C.S. Liao, C.H. Yan, Chin. Sci. Bull. 46 (2001) 1873.
- [53] D. Mandal, A. Datta, S.K. Pal, K. Bhattacharyya, J. Phys. Chem. B 102 (1998) 9070.
- [54] W.W. Stewart, J. Am. Chem. Soc. 103 (1981) 7615.
- [55] T.N. Burai, D. Panda, A. Datta, Chem. Phys. Lett. 455 (2008) 42.
- [56] T.N. Burai, T.K. Mukherjee, P. Lahiri, D. Panda, A. Datta, J. Chem. Phys. 131 (2009) 34504–34511.
- [57] P. Midoux, P. Wahl, J.C. Auchet, M. Monsigny, Biochim. Biophys. Acta. 801 (1984) 16.
- [58] J.R. Lakowicz, Principles of Fluorescence Spectroscopy, 3rd Ed, Springer, 2006.
- [59] D.M. Togashi, S.M.B. Costa, New J. Chem 26 (2002) 1774–1783.
- [60] S.K. Pal, J. Peon, A.H. Zewail, Proc. Natl. Acad. Sci. USA 99 (2002) 1763.
- [61] K.J. Laidler, J. Chem. Phys. 90 (1989) 151.
- [62] A.K. Michael, J. Wlodzimier. J.K. Tai. F1768.
- [63] S. Ghosh, K. Sahu, S.K. Mondal, P. Sen, K. Bhattacharyya, J. Chem. Phys. 125 (2006) 054509.
- [64] A. Ahmad, T. Kurkina, K. Kern, K. Balasubramanian, Chem. Phys. Chem 10 (2009) 2251.
- [65] S. Ghosh, S.K. Mondal, K. Sahu, K. Bhattacharyya, J. Phys. Chem. A 110 (2006) 13139.
- [66] E.L. Quitevis, A.H. Marcus, M.D. Fayer, J. Phys. Chem. 97 (1993) 5762.
- [67] N.C. Maiti, M.M.G. Krishna, P.J. Britto, N. Periasamy, J. Phys. Chem. B 101 (1997) 11051.